Journal of Nuclear Medicine, published on August 28, 2020 as doi:10.2967/jnumed.120.248500

Dopaminergic nigrostriatal connectivity in early Parkinson disease: *in vivo* neuroimaging study of ^{11}C-DTBZ PET combined with correlational tractography.

Short running title: Nigrostriatal connectivity in PD.

Carlos A. Sanchez-Catasus [1,2,3], Nicolaas I. Bohnen[1,3,4.5], Fang-Cheng Yeh[6], Nicholas D'Cruz[7], Prabesh Kanel[1,3], Martijn L.T.M. Müller[1,3]

[1]Department of Radiology, Division of Nuclear Medicine, University of Michigan Health System, Ann Arbor, MI, USA.

[2]Department of Nuclear Medicine and Molecular Imaging, University Medical Center Groningen, Groningen, Netherlands.

[3]Morris K. Udall Center of Excellence for Parkinson's Disease Research, University of Michigan, Ann Arbor, MI, USA.

[4]Department of Neurology, University of Michigan Health System, Ann Arbor, MI, USA.

[5]Neurology Service and GRECC, Veterans Administration Ann Arbor Healthcare System, Ann Arbor, MI, USA.

[6]Department of Neurological Surgery, University of Pittsburgh, Pittsburgh, PA, USA.

[7]Department of Rehabilitation Sciences, KU Leuven, Leuven, Belgium.

Corresponding author: Martijn L.T.M. Müller; Domino's Farms, Suite B1200 24 Frank Lloyd Wright Dr. Ann Arbor, MI 48106; Phone: 734- 998-8400; Fax: 734-998-8403; E-mail: mtmuller@umich.edu

First author: Carlos A. Sanchez-Catasus; Domino's Farms, Suite B1200 24 Frank Lloyd Wright Dr. Ann Arbor, MI 48106; Phone: 734-998-7195; Fax: 734-998-8403; E-mail: carlosas@umich.edu, casanchezcatasus@gmail.com

Abstract

Previous histopathological and animal studies have shown axonal impairment and loss of connectivity of the nigrostriatal pathway in Parkinson disease (PD). However, there are conflicting reports from *in vivo* human studies. ^{11}C-dihydrotetrabenazine (^{11}C-DTBZ) is a vesicular monoamine type 2 transporter PET ligand that allows assessment of nigrostriatal presynaptic dopaminergic terminal integrity. Correlational tractography based on diffusion magnetic resonance imaging can incorporate ligand-specific information provided by ^{11}C-DTBZ PET into the fiber tracking process. The purpose of this study was to assess the *in vivo* association between the integrity of the nigrostriatal tract (defined by correlational tractography) and the degree of striatal dopaminergic denervation based on ^{11}C-DTBZ PET. **Methods:** The study involved 30 subjects with mild to moderate PD (23 males; 7 females; mean age 66 ± 6.2 years, disease duration: 6.4 ± 4.0 years; Hoehn and Yahr stage: 2.1 ±0.6; MDS-revised UPDRS (I -III) total score: 43.4 ± 17.8) and 30 control subjects (18 males; 12 females; mean age 62 ± 10.3 years). ^{11}C-DTBZ PET was performed using standard synthesis and acquisition protocols. Correlational tractography was performed to assess quantitative anisotropy (QA; a measure of tract integrity) of white matter fibers correlating with information derived from striatal ^{11}C-DTBZ data using the DSI Studio toolbox. Scans were re-aligned according to least (LA) and most clinically affected (MA) cerebral hemispheres. **Results:** Nigrostriatal tracts were identified in both hemispheres of PD patients. Higher mean QA values along the identified tracts were significantly associated with higher striatal ^{11}C-DTBZ DVR values (*LA: r= 0.57; p= 0.001;* MA *r= 0.44; p= 0.02*). Lower mean QA values of the identified tract associated with increased severity of bradykinesia features derived from MDS-UPDRS clinical rating scale in the LA hemisphere (*r= -0.42; p= 0.02*). Cross-validation revealed the generalizability of these results.

Conclusions: These findings suggest that impaired integrity of dopaminergic nigrostriatal nerve terminals is associated with nigrostriatal axonal dysfunction in mild to moderate PD. Assessment of nigrostriatal tract integrity may be suitable as a biomarker of early or even prodromal stage PD.

Key words: Parkinson disease; dopaminergic nigrostriatal connectivity; ^{11}C-DTBZ PET; correlational tractography; diffusion magnetic resonance imaging.

Introduction

A key pathological hallmark of Parkinson disease (PD) is the loss of dopamine producing neurons in the substantia nigra (SN) pars compacta in the setting of alpha-synucleinopathy (*1-3*). This progressive pathological process in the SN results in dopaminergic losses in the striatum that associate with disease-specific motor impairments (*2,3*). However, less is known about concurrent degeneration of axons that project to the striatum.

There are a multitude of PET and SPECT radiotracers to assess nigrostriatal presynaptic terminal integrity (*4*). ^{11}C-dihydrotetrabenazine (^{11}C-DTBZ) is a radioligand for the vesicular monoamine transporter type 2 (VMAT2). VMAT2 is the protein responsible for pumping monoamines from cytosol into synaptic vesicles. ^{11}C-DTBZ is particularly useful as a marker of the striatal dopaminergic terminal since it is less influenced by compensation or pharmacological regulation (*5*) and has high dopaminergic specificity in the striatum (*6*). Various diffusion magnetic resonance imaging (dMRI) methods are available that allow for identification of white matter tracts and provide metrics to assess their microstructural integrity. These methods include diffusion tensor imaging (DTI) (*7*), generalized q-sampling imaging (GQI) (*8*), and q-space diffeomorphic reconstruction (QSDR) (*9*).

Previous histopathological and animal studies suggest that synaptic and axonal abnormalities may even occur before degenerative loss of neuronal cell bodies in PD (*for review see 10*). However, there have been conflicting reports about the association between striatal dopaminergic deficits and nigrostriatal tract integrity. Two DTI and dopamine transporter SPECT imaging studies with large patient cohorts found that fractional anisotropy (FA) in the SN decreased with increasing dopaminergic deficits as measured by putaminal dopaminergic binding ratios (*11, 12*).

A recent clinicopathological study, however, found no association between striatal dopamine transporter binding and the number of postmortem striatal axons in fourteen confirmed PD subjects (*13*). The latter finding may be explained by the relatively long time-interval between the *in vivo* imaging and *ex vivo* pathological assessments (5.2 ± 3.4 years). Two other studies using DTI-based brain tractography, one in fifty subjects with PD (*14*) and the other in sixteen non-human primates with unilateral nigrostriatal MPTP-induced injury (*15*), did not find a significant correlation between PET (*15*) or SPECT (*14*) and diffusion measures such as FA, axial, radial or mean diffusivities. In these two studies, probabilistic tracking was carried out to identify the nigrostriatal tract in each study subject using dMRI followed by linear regressions to correlate diffusion measures and the molecular imaging measures.

We postulate that tractographic reconstruction of the nigrostriatal dopaminergic pathway by simultaneously integrating additional information provided by PET or SPECT measurements of striatal presynaptic dopaminergic terminals may help to identify a more reliable nigrostriatal dopaminergic tract.

Correlational tractography has recently been developed as a novel alternative method that adopts the "correlation tracking" paradigm, using a non-parametric permutation test to search for the association of white matter fibers with a specific variable of interest (*16*). Therefore, it is possible to incorporate PET molecular information into the fiber tracking process so that the pathway only includes those white matter fibers that are specifically related to the PET information. Correlational tracking is achieved using QSDR algorithm (*8*), which is a generalization of the GQI method and allows tractography in a common stereotactic space (e.g. MNI space). One quantitative measure that can be derived from GQI is quantitative anisotropy

(QA) (*8*). QA measures the density of anisotropic diffusion water, a metric of integrity for each fiber population (9), and may provide a more reliable microstructural integrity metric compared to standard diffusion measures (*17, 18*). Correlational tracking of nigrostriatal dopaminergic fibers with QA can be used in a first step to identify a group-based "tract template" using the PET information of the dopaminergic presynaptic terminal. In a second step, the mean QA extracted from each subject across the template can be used as a measure of the whole tract integrity, suitable for assessing its association with the dopaminergic nerve terminal at the individual level.

The purpose of the present study is to assess the association between nigral white matter projections and the degree of striatal dopaminergic denervation, using combined analysis based on *in vivo* ^{11}C-DTBZ PET and dMRI correlational tractography using QA. We hypothesize that the degree of striatal dopaminergic degeneration is associated with compromised integrity of nigral white matter tracts in early PD.

Materials and Methods

Subjects

Thirty subjects with PD (23 men; 7 women; mean age 66 ± 6.2 years) were selected from ongoing studies at our center. Participant selection was based on three criteria: 1) only subjects with mild to moderate PD (Hoehn and Yahr (HY) stage ≤ 3) were included in order to avoid a possible floor effect associated with severe nigrostriatal dopaminergic denervation; 2) high quality reconstruction of dMRI, as evaluated by R^2 value between the subject QA map and the QA MNI map (> 0.70, see below for details); and 3) a time interval between clinical

examinations and neuroimaging assessments of 2 months or less to ensure no significant clinical interval changes. The study also included thirty age- and gender-matched healthy control subjects (18 men; 12 women; mean age 62 ± 10.3 years), with similar constraints as described in criteria #2 and #3 above.

All patients met the UK Parkinson's Disease Society Brain Bank clinical diagnostic criteria for PD (*19*). This was further confirmed by the presence of a typical pattern of striatal dopaminergic denervation on ^{11}C-DTBZ brain PET (*6*). The Movement Disorder Society-revised Unified Parkinson's Disease Rating Scale (MDS-UPDRS) examination was performed in all PD subjects to provide measures of clinical symptom severity (*20*). We used the bradykinesia sub-score derived from MDS-UPDRS part III - which is the best cardinal motor predictor of nigrostriatal dopaminergic deficit in PD (*21*) to examine clinical correlates of the correlational tractography findings. The motor examination was performed in the dopaminergic medication 'off' state in the morning after overnight withdrawal, except for one de-novo patient. In 19 PD subjects, clinical motor symptoms were predominantly on the right side of the body and in the other 11 PD subjects these symptoms were predominantly on the left side. Table 1 summarizes main demographic and clinical characteristics of all participants.

The study was approved by the Institutional Review Boards of the University of Michigan School of Medicine and Veterans Affairs Ann Arbor Healthcare System. Written informed consent was obtained from all subjects prior to any research procedures.

^{11}C-DTBZ PET acquisition and preprocessing

PET imaging was performed in 3D imaging mode using an ECAT Exact HR+ tomograph (Siemens Molecular Imaging, Inc.). A detailed description of PET images preprocessing can be found elsewhere (*22*).

^{11}C-DTBZ [no-carrier-added (+)-α-11C-dihydrotetrabenazine] was prepared using high-specific activity ^{11}C-methyl iodide as reported previously (*23*). ^{11}C-DTBZ PET scans were performed using a bolus/infusion protocol acquiring 15 emission scans over 60 min (4 × 30 s; 3 × 1 min; 2 × 2.5 min; 2 × 5 min; 4 × 10 min), with a priming bolus of 55% followed by continuous infusion of the remaining 45% over the study duration using a dose of 555 MBq.

All dynamic PET imaging frames were spatially co-registered within subjects with a rigid body transformation to reduce the effect of subject motion during the imaging session (*24*). These motion-corrected PET frames were spatially co-registered to anatomical magnetic resonance image (MRI) using SPM8 software (Wellcome Trust Centre for Neuroimaging, London, UK). IDL image analysis software (Research systems, Inc) was used to manually trace volumes of the striatum (and sub-regions) of both cerebral hemispheres on the MRI scan. Striatal ^{11}C-DTBZ distribution volume ratio (DVR), a measure of dopaminergic binding, was estimated by using the Logan graphical analysis method (*25*) with the striatal time-activity curves as the target regions and neocortex as the reference input.

MRI acquisition and preprocessing

All subjects underwent high-resolution structural brain MRI (3D T1-weighted) for anatomical co-registration with the PET scan. MRI was performed on a 3T Philips Achieva system (Philips)

using an eight-channel head coil. A detailed description of structural brain MRI acquisition parameters can be found elsewhere (*22*).

During the same visit, dMRI was obtained for correlational tractography (TR/TE=8700/70 ms, 1.75 mm x 1.75 mm x 2mm, 15 diffusion sampling directions, b-value= 800 s/mm2). In a subsequent step, each volume was registered to the B0 volume using an affine transform with mutual information as a cost function. Preprocessing was then carried out in MRtrix (version 3.0_RC3) (*26*) including denoising (*27*), removal of Gibbs ringing artefacts (*28*) and correction of motion and eddy-current distortion (*29*). During the distortion correction, outlier replacement (*30*) and slice-to-volume correction of intra-volume movement (*31*) was performed.

Quality control of the preprocessed dMRI data was performed using DSI-studio toolbox (http://dsi-studio.labsolver.org). The b-table was checked by an automatic quality control routine to ensure its accuracy. Image dimension, resolution, and b-table were consistent between repeated scans. The neighboring DWI correlation was high and similar across all dMRI volumes (0.89 ± 0.01), indicating very good quality of preprocessed dMRI data relative to motion artifacts and low signal-to-noise ratio.

Neurological examinations, PET, and MRI were performed within a one-week interval in forty-nine (twenty-five controls) of sixty study subjects (82%). In four subjects (two controls) this interval was one month and in the remaining seven subjects (two controls) it was two months.

Connectometry databases

For correlational tractography analysis, three connectometry databases were created using DSI-Studio (http://dsi-studio.labsolver.org). Two databases included each study group (PD and

control databases, respectively) and a third included a combined group to explore whether the analysis of this group provides more robust estimates of nigrostriatal tracts (Supplementary Material).

In the PD group, we first flipped (right to left) the dMRI images of the 11 patients with a left predominance of clinical symptoms. This was done to create a more uniform sample given the typical clinical motor symptom and striatal ^{11}C-DTBZ DVR asymmetry in PD, at least in early disease stages (*6*). Therefore, the left hemisphere was represented as the "most affected" hemisphere (MA) in all patients and the right hemisphere as the "least affected" (LA).

The dMRI preprocessed data in each group were reconstructed in the MNI space using QSDR to obtain the spin distribution function (SDF) (*8,9*). QSDR first calculates QA mapping (defined on SDF) in the native space and then normalizes it to the MNI QA map. The reconstruction was performed using a customized template of 62 control healthy subjects from our laboratory's ongoing studies (age=64.6 ±9.8 years; 31 females and 31 males), different from the control group described above, since the use of an age-matched template is more appropriate than the DSI studio default template (based on young adults only). Details of template creation can be found in the Supplementary Material. A diffusion sampling length ratio of 0.5 was used. The diffusion was quantified using restricted diffusion imaging (*32*). QA was extracted as the local connectome fingerprint (*17*) and used in the correlational tractography.

The quality of post reconstruction was tested in all subjects by using the R^2 value between the subject QA map and the QA MNI map. The average of R^2 was 0.82 ± 0.02 (min = 0.74, max = 0.85) representing a very good registration quality, in accordance with DSI-studio standard (http://dsi-studio.labsolver.org).

Correlational tractography combined with ^{11}C-DTBZ PET

Selecting the functional striatal region for correlational tracking

To determine the optimal DTBZ values for correlational tracking of PD, control and combined groups, an exploratory analysis of the ^{11}C-DTBZ DVR values of the whole striatum and its sub-regions was performed. We used striatal sub-regions based on a previous work in our laboratory (*33*). Requirements for the ^{11}C-DTBZ DVR values were to meet the following four criteria: 1) The values must follow a normal distribution or at least one histogram with a single peak in the combined group. Otherwise, it would be more appropriate to perform the analysis only in separate groups. This criterion ruled out the whole striatum for analysis since in both hemispheres its histograms had two peaks (Supplementary Figure 1); 2) The values of the selected sub-region must be collinear with the values of the whole striatum (the dopaminergic terminal); 3) The values must have a similar coefficient of variation (CoV) in both hemispheres. This criterion was to ensure that the possible different results in each hemisphere were not due to differences in the variability of ^{11}C-DTBZ DVR values; and 4) Left-right asymmetry of the values should be as small as possible in the PD group. This criterion served to avoid that the possible asymmetry in the tracts was due only to the asymmetry in the ^{11}C-DTBZ DVR values rather than the relationship of each tract with its dopaminergic terminal. Results of this exploratory analysis showed that the anteroventral striatum (AVS) was the best striatal sub-regions in meeting all four criteria: normal distribution in both hemisphere (Supplementary Figure 1); Collinearity with the whole striatum (Supplementary Tables 1-3); Similar CoV (Supplementary Tables 4-6); and the lowest mean asymmetry (Supplementary Figure 2). It is

important to note that the AVS was not relevant due to its anatomical location but rather to its functional relevance to guide the tract reconstruction with "dopaminergic" specificity.

Tracking the nigrostriatal dopaminergic pathway

The connectometry databases were used to track the correlation of AVS ^{11}C-DTBZ DVR on QA using a deterministic fiber tracking algorithm (*18*), with the SN as the seeding region and the whole striatum as the terminative region, corresponding to each cerebral hemisphere. Linear regression models were performed for each cerebral hemisphere with a T-score threshold of 3. The SN and the striatum were defined using the ATAG basal ganglia atlas (*34*). Age and gender were considered in the linear regression as nuisance covariates. Topology-informed pruning was conducted with 2 iterations to remove false connections (*35*). All tracts generated from bootstrap resampling were included. A false discovery rate (FDR) threshold of 0.05 was used to select tracts. The seeding number for each permutation was 100,000. To estimate the FDR, 4,000 randomized permutations were applied to the group label to obtain the null distribution of the tracts length. Tracts identified in each hemisphere were defined as their respective tract templates. Subsequently, the mean QA across the whole template (of each hemisphere) was extracted in every subject and used to assess the correlation with the corresponding whole striatum ^{11}C-DTBZ DVR values. Tract volumes were also extracted.

We performed a complementary analysis by repeating the same analyses described above using the dMRI FA index (Supplementary Material), as this metric has been commonly used in prior studies. For this analysis the T-score threshold was lowered to 2 to track the correlation with the AVS ^{11}C-DTBZ DVR on FA because no tracts showed significant correlation using a more

conservative T-score threshold. For both QA and FA analyses, the resulting tracts were identified by using the HCP842 tractography atlas (*36*).

Shapiro-Wilk W test showed normal distribution for all main study variables (Supplementary Table 7).

Statistical analysis

Association between tract integrity and dopaminergic terminal.

Pearson correlation was used to assess the association of mean QA values across the identified tract templates with whole striatum ^{11}C-DTBZ DVR values.

Cross-validation

To assess the generalizability of the estimated tracts in the PD group, we performed a cross-validation using the leave-one-out (LOO) methodology. The training set was defined as the mean QA extracted in each PD subject from the tract template using the PD group (for each hemisphere). To get the validation element of a single PD subject, we constructed a new tract template but leaving that specific PD subject out. This new tract template was used to extract the mean QA from that PD subject (mean QA-LOO). This process was repeated for each of the 30 PD subjects (for each hemisphere).

As a measure of fit and to summarize the error between the data (mean QA-LOO of each PD subject) and the model (mean QA of each PD subject from the tract template using the PD group), the root mean squared error (RMSE) was used. Pearson correlation was used to assess

the association of mean QA- LOO and the corresponding AVS and whole striatum ^{11}C-DTBZ DVR values.

Association between tract integrity and motor symptoms (bradykinesia)

Pearson correlation was used to evaluate the association of mean QA values (and mean QA-LOO) with the MDS-UPDRS bradykinesia sub-score, for both hemispheres in the PD group.

Group comparisons

Mean QA and whole striatum ^{11}C-DTBZ DVR values between group (for each hemisphere) were compared using the Student's t-test for independent samples. We also compared those values between hemisphere in the PD group (LA vs. MA) and in the control group using the paired Student's t-test. The mean QA values used for these analyzes were extracted using tract templates from the combined group analysis (Supplementary Material) as no tracts were identified in the control group in separate analyses.

For comparison and complementary analyses purposes, we also performed the same statistical analyses described above (except cross-validation) for correlational tractography analysis using the FA dMRI metric.

Statistical analyses were carried out using STATISTICA software (Stat Soft, Inc., version 8.0). The significance level was set at $p < 0.05$. For the three correlation tests (related to mean QA or mean QA-LOO) in the same hemisphere in the PD group, we computed 95 % and 98.33 % percentiles bootstrap CI. The latter implicitly considers the p-values for multiple comparisons.

For the comparison tests between groups (and between hemispheres), we considered a Bonferroni-corrected significant p-value of 0.00625 (0.05 / 8 comparison tests).

Results

Tract templates and association of tracts integrity with dopaminergic terminals.

Figure 1.A shows tract templates identified in the PD group. The LA hemisphere tract originated slightly below the posterior part of the SN, converged to the anterior dorsal part of the SN, traveled upwards passing very close to the subthalamic nucleus, then turned laterally above the subthalamic nucleus reaching a white matter region between the anterior putamen and the posterior aspect of the caudate nucleus. This tract also corresponded to a small segment of the right frontopontine tract as defined by the HCP842 tractography atlas (*36*). The tract volume was 1.9 cm^3. The MA hemisphere tract followed a similar path, although its volume was smaller (1.02 cm^3) and did not reach the striatum. The mean QA was positively correlated with the whole striatum ^{11}C–DTBZ DVR values in both hemispheres (Figs. 1.B and 1.C, Table 2).

Statistically significant tract templates could not be identified in the control group in either hemisphere. Complementary analyses in the combined group confirmed these findings in the control group (Supplementary Figure 3).

Similar to the QA index, the analysis based on the FA index did not identify tract templates in the control group, whereas in the PD group it was only identified in the LA hemisphere (Supplementary Figure 4.A). The mean FA was positively correlated with whole striatum ^{11}C–DTBZ DVR values in the LA hemisphere (Supplementary Figure 4.B) but these correlations were lower compared to those observed using mean QA in the same hemisphere.

Complementary analyses in the combined group confirmed the negative results in the control group using FA (Supplementary Figure 5).

Cross-validation

Figures 2.A and 2.B show the relation between the data and the model in the PD group in both hemispheres (MA and LA) as described above. RMSE was low in both cases (MA: 4.52×10^{-4}; LA: 4.29×10^{-4}). However, the correlations of the mean QA-LOO with the whole striatum DTBZ DVR values were only significant in the LA hemisphere (Figs 2.C and 2.D, Table 3), indicating its generalizability to independent datasets.

Association between tract integrity and bradykinesia

Both the mean QA and the mean QA-LOO in the LA hemisphere were significantly negatively correlated with the bradykinesia sub-score of PD subjects (Figs 3.B and 3.D, Tables 2 and 3, respectively). Using the mean FA, the correlation was also found in the LA hemisphere (Supplementary Figure 6) but was much lower than the QA findings in the same hemisphere (Figs. 3.B and 3.D).

Group comparisons

Comparison with normal controls showed that striatal PET measures were indicative of neurodegeneration in PD patients, as well as the mean QA across subjects in both hemispheres (Table 4, Supplementary Figure. 7.A). There were no significant differences between hemispheres in the control group, except for the mean QA, which could be explained by the differences between the left and right tract templates of the combined group (Supplementary

Figure 3.A) applied to the control group. As expected, striatal ^{11}C-DTBZ DVR and mean QA in the LA hemisphere in the PD group was significantly higher compared to the MA hemisphere.

Using FA, there were no significant differences between PD and control groups for mean FA across subjects. Furthermore, the mean FA across the PD patients was not significantly different between hemispheres (Supplementary Figure 7.B).

Discussion

The aim of this study was to examine the association between the integrity of nigrostriatal white matter projections and striatal dopaminergic (VMAT2) nerve terminal integrity in PD patients with mild to moderate disease severity. Integrated neuroimaging analysis using ^{11}C-DTBZ PET and correlational tractography identified a bundle of fibers (tract) in each cerebral hemisphere in PD patients, extending from the SN to the striatum in the least affected (LA) hemisphere, with a smaller tract identified in the most affected (MA) hemisphere. Lower mean QA values of the identified tracts, reflecting more impaired axonal integrity, were associated with decreased striatal dopaminergic binding in both hemispheres. Moreover, the mean QA difference between both hemispheres suggests a "continuum" from a less advanced (LA tract) to a more advanced (MA tract) stage of the disease. The integrated dMRI-PET definition of these tracts increases the reliability that the identified tracts are dopaminergic in nature. Furthermore, the path of the LA-hemisphere tract closely resembles the known anatomy of the nigrostriatal pathway (*37*). Lower mean QA values of the LA-hemisphere tract were also associated with increased severity of bradykinesia clinical ratings in the PD subjects. This finding supports our interpretation of the relevance of this pathway in the pathophysiology of PD. We were able to cross-validate the LA-hemisphere tract suggesting generalizability of our findings. Taken together, these findings show

that striatal dopaminergic degeneration is associated with the integrity of the dopaminergic nigrostriatal pathway, at least in the setting of mild to moderate dopaminergic losses in PD. Our findings also suggest that ^{11}C-DTBZ PET may reflect axonal dysfunction in these patients.

Our findings are in line with previous observations in histopathological and animal studies that Lewy bodies accumulate in axons and presynaptic striatal nerve terminal, resulting in axonal impairment and gradual loss of connectivity of the nigrostriatal pathway in PD (for a review see *10*). For example, Braak et al. showed that alpha-synuclein deposits were not only present in Lewy body inclusions within the cell body, but were also present in axonal projections (*38*).

Our study showed the advantage of integrating information from both tractography and molecular PET data to define dopaminergic white matter fibers. Unlike prior studies using standard diffusion measures such as FA, we used QA as a measure of local fiber integrity (*17*). The main disadvantage of using diffusivity metrics (such as FA) is that restricted and less-restricted diffusion are mixed due to Brownian motion. In contrast, QSDR quantifies the density of restricted and less-restricted diffusion for each fiber population (fiber-specific within a voxel), while in FA all fiber populations within a voxel will share the same measurement. QA as the fingerprint of the local connectome is more sensitive to individual differences compared to standard diffusion measures (*17*). This concept is consistent with a previous study suggesting that QA may contribute to more reliable tractography (*39*). Notably, by using FA no tract was identified in the MA hemisphere, even using a less conservative T-score threshold, and no significant differences were found for mean FA between control and PD groups (Supplementary Figure 7.B). Our study also showed that correlational tracking using QA yielded clinically relevant correlations (bradykinesia ratings); findings that were less robust for the FA index. The

use of standard tractography based on using dMRI data alone and the relative disadvantages of the standard diffusion measures may explain the negative findings of previous studies (*14, 15*).

Our findings support the use of AVS ^{11}C-DTBZ DVR values for correlational tracking to guide the tract reconstruction with "dopaminergic" specificity. The innervation of AVS originates not only from the ventral tegmental area, but also includes projections from the SN (for review see 40), hence explaining the dopaminergic collinearity of the AVS with the whole striatum.

Nigrostriatal white matter tracts could not be reconstructed for the control group. This could be explained by the absence of a pathophysiological process affecting axons in healthy older adults. Indeed, our results showed that the mean QA values of the tracts in PD patients were significantly lower compared to the controls, suggesting that nigrostriatal pathway integrity is preserved in the control group. Therefore, our approach appears sensitive to SN and nigrostriatal pathway pathology. In healthy controls, possible degeneration of the SN, for example due to aging (*41*), is much weaker and our approach is unable to capture it. Future studies are needed to include subjects in the prodromal phase of PD to further evaluate the relative timing of nigrostriatal axonal and striatal end terminal neurodegenerative processes.

The smaller size of the tract identified in the MA hemisphere suggests that there are fewer axons between the SN and the striatum in that hemisphere. Our findings also suggest that there may be a time window to visualize the nigrostriatal dopaminergic pathway using our approach. This window encompasses the mild to moderate stages, and perhaps the prodromal phase.

Our cross-sectional data in a symptomatic PD population do not allow assessment of the temporal order of axonal and presynaptic degenerations, since it requires longitudinal

observations in a sample that also includes subjects in the prodromal phase of PD. However, our results suggest that synaptic and axonal degeneration may occur to some extent in parallel (mean QA and striatal DTBZ are interrelated) although possibly at a different rate and eventually affecting the survival of dopaminergic cell bodies in the SN.

Our study has several limitations. Although a particular strength of correlational tractography with ^{11}C-DTBZ PET is that it selectively allows for parcellation of dopaminergic pathways, we cannot rule out that the identified tracts also included some non-dopaminergic fibers. However, the clinical correlation of tract integrity in the least affected hemisphere with the clinical bradykinesia measure, suggest that a relatively high percentage of the white matter fibers included in this tract were probably dopaminergic fibers of the nigrostriatal pathway. Second, the identified tracts extend slightly below the SN. This is likely due to limitations in the spatial resolution of dMRI. Nonetheless, the LA tract path was close to the known anatomy of the nigrostriatal pathway (*37*).

Conclusions

The combined VMAT2 PET-dMRI correlational tractography approach showed that nigrostriatal white matter pathway integrity is associated with striatal dopaminergic denervation in mild to moderate PD and may explain the disease-defining motor impairment (bradykinesia). These findings also suggest that *in vivo* PET imaging with ^{11}C-DTBZ may reflect axonal dysfunction in PD. Assessment of nigrostriatal tract integrity may be most useful before the occurrence of severe striatal dopaminergic denervation. Therefore, our approach may be suitable as a biomarker of early stage or even prodromal phase PD. Further studies are needed to assess

whether changes in early nigrostriatal dopaminergic pathway integrity are associated with PD development and/or disease progression.

Disclosure:

The authors have nothing to disclose and no relevant conflict of interest.

Acknowledgments:

We want to thank Christine Minderovic, Cyrus Sarosh, Jacqueline Dobson, PET technologists, cyclotron operators and radiochemists. We also want to thank funding agencies: the NIH, the Department of Veterans Affairs and the Michael J. Fox Foundation. We express special thanks to our patients with PD and research volunteers without whom our work would not have been possible.

KEY POINTS:

QUESTION: Is striatal dopaminergic degeneration associated with the integrity of the white matter fibers corresponding to the nigrostriatal pathway in early Parkinson disease?

PERTINENT FINDINGS: In a cohort study, using combined analysis based on ^{11}C-DTBZ PET and correlational tractography, striatal dopaminergic degeneration was significantly associated with the integrity of the dopaminergic nigrostriatal pathway in 30 patients with mild to moderate Parkinson disease. These findings also suggest that ^{11}C-DTBZ PET may reflect axonal dysfunction in these patients.

IMPLICATIONS FOR PATIENT CARE: The assessment of nigrostriatal tract integrity may be suitable as a biomarker of early stage or even prodromal phase PD by combining ^{11}C-DTBZ PET and correlational tractography.

References

1. Spillantini MG, Schmidt ML, Lee VM, Trojanowski JQ, Jakes R, Goedert M.
   a. Alpha-synuclein in Lewy bodies. Nature. 1997;388:839-40.
2. Lang AE, Lozano AM. Parkinson's disease. First of two parts. N Engl J Med. 1998;339:1044-1053.
3. Lang AE, Lozano AM. Parkinson's disease. Second of two parts. N Engl J Med. 1998 ;339:1130-1143.
4. Liu ZY, Liu FT, Zuo CT, Koprich JB, Wang J. Update on Molecular Imaging in Parkinson's Disease. Neurosci Bull. 2018;34:330-340.
5. Vander Borght T, Kilbourn M, Desmond T, Kuhl D, Frey K. The vesicular monoamine transporter is not regulated by dopaminergic drug treatments. Eur J Pharmacol 1995, 294:
   a. 577–583.
6. Bohnen NI, Albin RL, Koeppe RA, et al. Positron emission tomography of monoaminergic vesicular binding in aging and Parkinson disease. J Cereb Blood Flow Metab. 2006;26:1198-1212.
7. Jellison BJ, Field AS, Medow J, Lazar M, Salamat MS, Alexander AL. Diffusion tensor imaging of cerebral white matter: a pictorial review of physics, fiber tract anatomy, and tumor imaging patterns. AJNR Am J Neuroradiol. 2004; 25:356-369.
8. Yeh FC, Wedeen VJ, Tseng WY. Generalized q-sampling imaging IEEE Trans Med Imaging. 2010;29:1626-1635.
9. Yeh FC, Tseng WY. NTU-90: a high angular resolution brain atlas constructed by q-space diffeomorphic reconstruction. Neuroimage. 2011; 58:91-99.

10. Bridi JC, Hirth F. Mechanisms of α-Synuclein Induced Synaptopathy in Parkinson's Disease. Front Neurosci. 2018;12:80. doi: 10.3389/fnins.2018.00080. eCollection 2018.
11. Zhang Y, Wu IW, Tosun D, Foster E, Schuff N, Parkinson's Progression Markers Initiative. Progression of Regional Microstructural Degeneration in Parkinson's Disease: A Multicenter Diffusion Tensor Imaging Study. PLoS One. 2016;11(10):e0165540.
12. Schuff N, Wu IW, Buckley S, et al. Diffusion imaging of nigral alterations in early Parkinson's disease with dopaminergic deficits. Mov Disord. 2015;30:1885-1892.
13. Honkanen EA, Saari L, Orte K, et al. No link between striatal dopaminergic axons and dopamine transporter imaging in Parkinson's disease. Mov Disord. 2019;34:1562-1566.
14. Zhang Y, Wu IW, Buckley S, et al. Diffusion tensor imaging of the nigrostriatal fibers in Parkinson's disease. Mov Disord. 2015;30:1229-1236.
15. Shimony JS, Rutlin J, Karimi M, et al. Validation of diffusion tensor imaging measures of nigrostriatal neurons in macaques. PLoS One. 2018;13(9):e0202201.
16. Yeh FC, Badre D, Verstynen T. Connectometry: A statistical approach harnessing the analytical potential of the local connectome. Neuroimage. 2016;125:162-171.
17. Yeh FC, Vettel JM, Singh A, et al. Quantifying Differences and Similarities in Whole-Brain White Matter Architecture Using Local Connectome Fingerprints. PLoS Comput Biol. 2016;12(11):e1005203.
18. Yeh FC, Verstynen TD, Wang Y, Fernández-Miranda JC, Tseng WY. Deterministic diffusion fiber tracking improved by quantitative anisotropy. PLoS One. 2013;8(11):e80713.

19. Hughes AJ, Daniel SE, Kilford L, Lees AJ. Accuracy of clinical diagnosis of idiopathic Parkinson's disease: a clinico-pathological study of 100 cases. J Neurol Neurosurg Psychiatry. 1992;55:181-184.
20. Goetz CG, Fahn S, Martinez-Martin P, et al. Movement Disorder Society-sponsored revision of the Unified Parkinson's Disease Rating Scale (MDS-UPDRS): Process, format, and clinimetric testing plan. Movement disorders: official journal of the Movement Disorder Society. 2007;22:41-47.
21. Vingerhoets FJ, Schulzer M, Calne DB, Snow BJ. Which clinical sign of Parkinson's disease best reflects the nigrostriatal lesion?Ann Neurol. 1997;41:58-64.
22. Müller ML, Albin RL, Kotagal V, et al. Thalamic cholinergic innervation and postural sensory integration function in Parkinson's disease. Brain 2013; 136:3282–3289.
23. Jewett DM, Kilbourn MR, Lee LC. A simple synthesis of [11C] dihydrotetrabenazine (DTBZ). Nucl Med Biol. 1997;24:197-199.
24. Minoshima S, Frey KA, Koeppe RA, Foster NL, Kuhl DE. A diagnostic approach in Alzheimer's disease using three-dimensional stereotactic surface projections of fluorine-18-FDG PET. J Nucl Med. 1995;36:1238-1248.
25. Logan J, Fowler JS, Volkow ND, Wang GJ, Ding YS, Alexoff DL. Distribution volume ratios without blood sampling from graphical analysis of PET data. J Cereb Blood Flow Metab. 1996;16:834-840.
26. Tournier JD, Smith R, Raffelt D, et al. MRtrix3: A fast, flexible and open software framework for medical image processing and visualisation. Neuroimage. 2019; 202:116137. doi: 10.1016/j.neuroimage.2019.116137. Epub 2019 Aug 29.

27. Veraart J, Novikov DS, Christiaens D, Ades-Aron B, Sijbers J, Fieremans E. Denoising of diffusion MRI using random matrix theory. Neuroimage. 2016;142:394-406.
28. Kellner E, Dhital B, Kiselev VG, Reisert M. Gibbs-ringing artifact removal based on local subvoxel-shifts. Magn Reson Med. 2016;76:1574-1581.
29. Andersson JLR, Sotiropoulos SN. An integrated approach to correction for off-resonance effects and subject movement in diffusion MR imaging. Neuroimage. 2016;125:1063-1078.
30. Andersson JLR, Graham MS, Zsoldos E, Sotiropoulos SN. Incorporating outlier detection and replacement into a non-parametric framework for movement and distortion correction of diffusion MR images. Neuroimage. 2016;141:556-572.
31. Andersson JLR, Graham MS, Drobnjak I, Zhang H, Filippini N, Bastiani M. Towards a comprehensive framework for movement and distortion correction of diffusion MR images: Within volume movement. Neuroimage. 2017;152:450-466.
32. Yeh FC, Liu L, Hitchens TK, Wu YL. Mapping immune cell infiltration using restricted diffusion MRI. Magn Reson Med. 2017;77:603-612.
33. Kwak, Y., Bohnen, N. I. , Müller, M. L. T. M. , Dayalu, P. , & Seidler, R. D. (2013). Striatal denervation pattern predicts levodopa effects on sequence learning in Parkinson's disease. Journal of Motor Behavior, 45, 423–429.
34. Keuken MC, Bazin PL, Crown L, et al. Quantifying inter-individual anatomical variability in the subcortex using 7 T structural MRI. Neuroimage. 2014;94:40-46.
35. Yeh FC, Panesar S, Barrios J, et al. Automatic Removal of False Connections in Diffusion MRI Tractography Using Topology-Informed Pruning (TIP). Neurotherapeutics. 2019;16(1):52-58.

36. Yeh FC, Panesar S, Fernandes D, et al. Population-averaged atlas of the macroscale human structural connectome and its network topology. Neuroimage. 2018;178:57-68.
37. Smith Y, Shink E, Sidibe M. Neuronal circuitry and synaptic connectivity
a. of the basal ganglia. Neurosurg Clin North Am. 1998;9:203-222.
38. Braak H, Sandmann-Keil D, Gai W, Braak E. Extensive axonal Lewy neurites in Parkinson's disease: a novel pathological feature revealed by alpha-synuclein immunocytochemistry. Neurosci. Lett 1999; 265: 67–69.
39. Zhang H, Wang Y, Lu T, et al. Differences between generalized q-sampling imaging and diffusion tensor imaging in the preoperative visualization of the nerve fiber tracts within peritumoral edema in brain. Neurosurgery. 2013;73:1044-1053.
40. Salgado S, Kaplitt MG. The nucleus accumbens: a comprehensive review. Stereotactic Funct Neurosurg (2015) 93(2):75–93.
41. Frey KA, Koeppe RA, Kilbourn MR, et al. Presynaptic monoaminergic vesicles in Parkinson's disease and normal aging. Ann Neurol. 1996;40:873-884.

Figures with legends

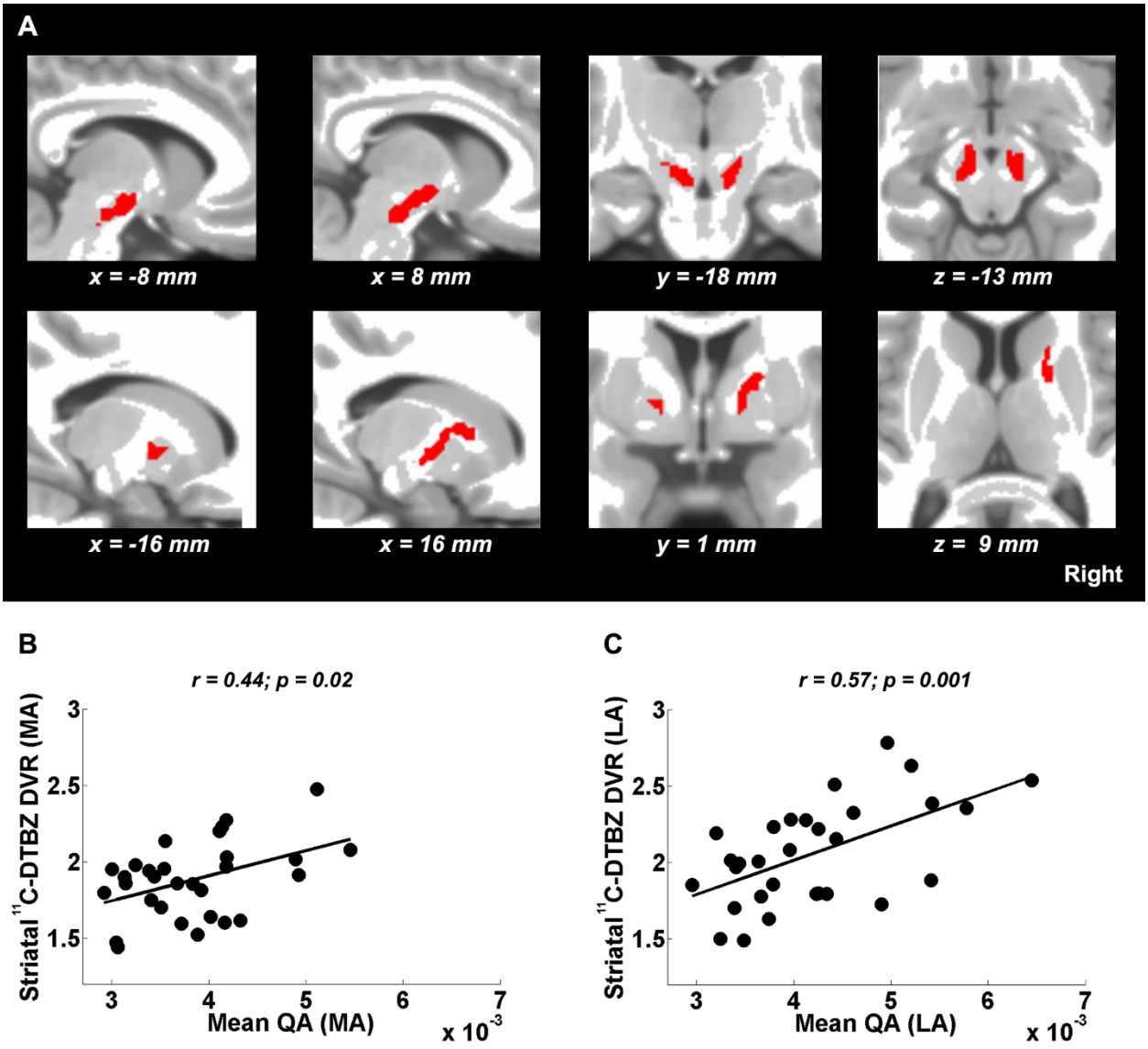

Figure 1. (A) Tract templates identified in the PD group in the most affected (MA, left side) and least affected (LA, right side) hemispheres (overlaid on a T1-weighted MR image in MNI space). **(B)** The mean QA (across the PD template) positively correlates with whole striatum ^{11}C–DTBZ DVR values in the MA hemispheres. **(C)** The same as (B) for the LA hemisphere.

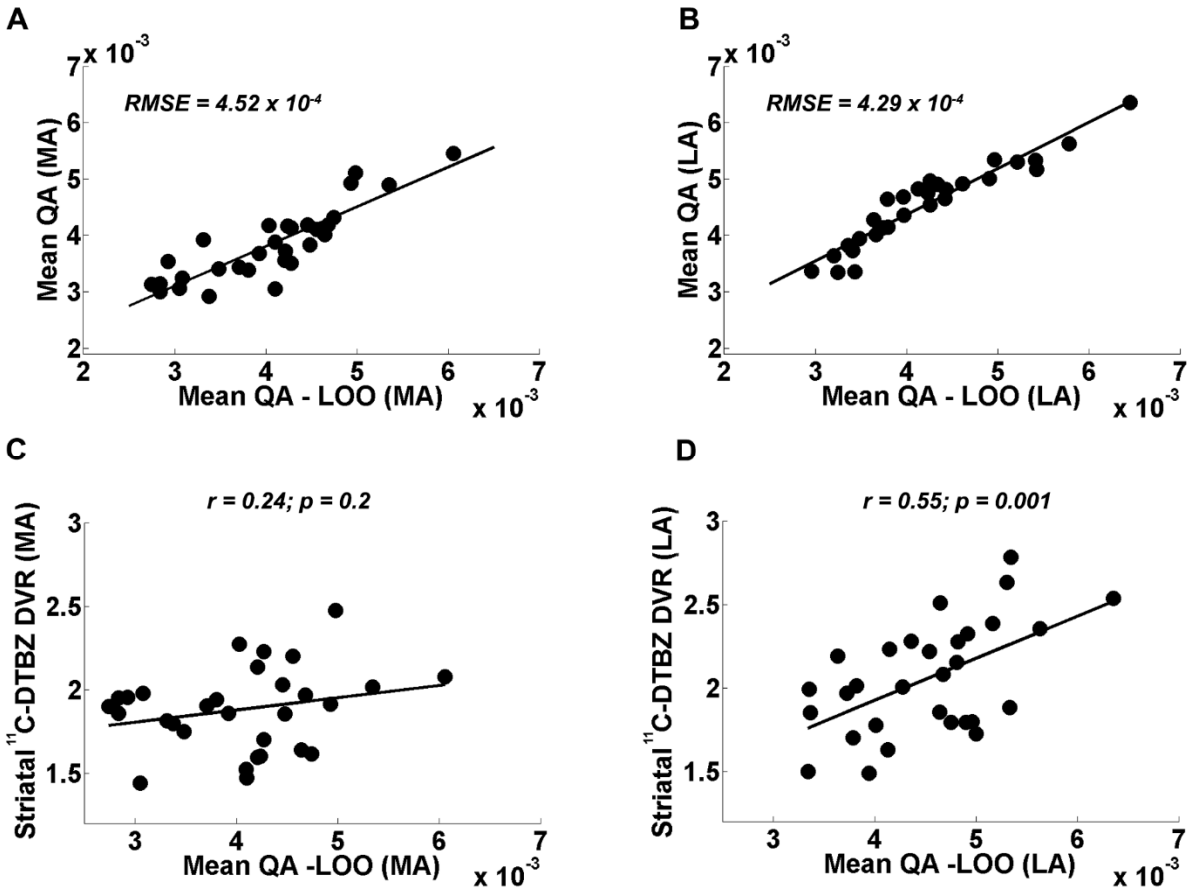

Figure 2. Relation between training and cross-validation sets using leave-one-out (LOO) approach (mean QA and mean QA-LOO, respectively) in MA **(A)** and LA **(B)** hemispheres of PD subjects. The root mean squared error (RMSE) was used as a measure of fit. **(C)** The mean QA-LOO did not correlate significantly with whole striatum ^{11}C–DTBZ DVR values in the MA hemisphere. **(D)** The same as **(C)** for the LA hemisphere but showing significant positive correlations. The MA (left) hemisphere in the PD group refers to the hemisphere clinically most affected in PD patients.

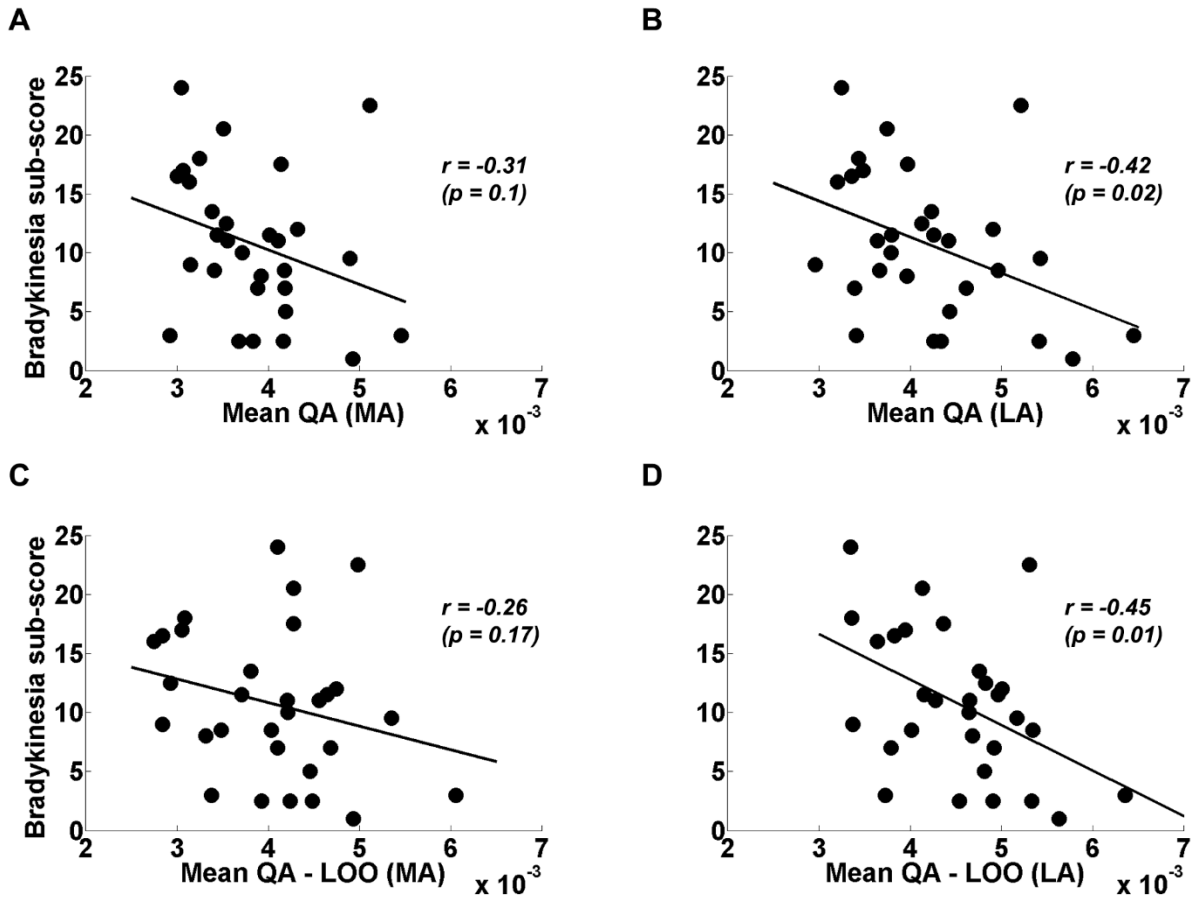

Figure 3. Relation between mean QA and MDS-UPDRS bradykinesia sub-score in the MA **(A)** and LA hemispheres **(B)** of PD patients. (**C**) and (**D**) the same as **(A)** and **(B)**, respectively, for mean QA-LOO**.** Mean QA **(B)** and mean QA-LOO **(D)** in the LA hemisphere were significantly negatively correlated with the bradykinesia sub-score. Mean QA-LOO is the mean QA of the individual tract of each PD patient as a result of leave-one-out (LOO) cross-validation. The MA (left) hemisphere in the PD group refers to the hemisphere clinically most affected in PD patients.

TABLES

TABLE 1. Demographic and clinical characteristics of PD and control subjects.

	PD (n=30)	**Control (n=30)**	**Statistical Significance**
Age (years)	66.0 ± 6.2	62.0 ± 10.3	t = 1.8 ; n.s.
Sex (males/females)	23/7	18/12	$\chi 2 = 1.9$; n.s.
Handedness (right/left)	27/3	26/4	$\chi 2 = 0.16$; n.s.
Bradykinesia sub-core*	10.7 ± 6.2	-	-
MDS-UPDRS (part I)	5.2 ± 17.8	-	-
MDS-UPDRS (part II)	5.8 ± 3.6		
MDS-UPDRS (part III)	32.4 ± 14.4	-	-
MDS-UPDRS (I -III) total score	43.4 ± 17.8	-	-
Hoehn and Yahr stage	2.1 ± 0.6	-	-
	(2; 1-3)†		
Motor disease duration (years)	6.4 ± 4.0	-	-
MoCA	27.7 ± 2.0		
Levodopa equivalent dose	573.6 ± 351.1		

*derived from MDS-UPDRS (part III). †In brackets, median; minimum –maximum of Hoehn and Yahr stage. MoCA= Montreal Cognitive Assessment.

TABLE 2. Correlation of mean QA with whole striatum ^{11}C-DTBZ DVR and bradykinesia sub-score in the PD group.

	Striatum		***Bradykinesia***	
	MA*	***LA†***	***MA***	***LA***
Pearson Coeff. (p-values)	*0.44 (0.02)*	*0.57 (0.001)*	*-0.31 (0.1)*	*-0.42 (0.02)*
95 % CI	*0.12, 0.68*	*0.33, 0.73*	*-0.72, 0.13*	*-0.71, -0.02*
98.33 % CI	*-0.04, 0.71*	*0.21, 0.78*	*-0.75, 0.24*	*-0.75, 0.02*

MA*(LA†) = clinically most (least) affected hemisphere in PD patients.

TABLE 3. Correlation of mean QA-LOO with whole striatum ^{11}C-DTBZ DVR and bradykinesia sub-score in the PD group using individual tracts as a result of cross-validation using leave-one-out (LOO) approach.

	Striatum		***Bradykinesia***	
	MA*	***LA†***	***MA***	***LA***
Pearson Coeff. (p-values)	*0.24 (0.2)*	*0.55 (0.001)*	*-0.26 (0.17)*	*-0.45 (0.01)*
95 % CI	*-0.06, 0.48*	*0.27, 0.74*	*-0.57, 0.12*	*-0.74, -0.02*
98.33 % CI	*-0.14, 0.50*	*0.16, 0.76*	*-0.61, 0.17*	*-0.78, -0.006*

MA* (LA†) = clinically most (least) affected hemisphere in PD patients.

TABLE 4. Comparison between control and PD groups for each brain hemisphere (and interhemispheric) of striatal ^{11}C-DTBZ DVR and mean QA.

	Control		**PD**		**Control vs. PD Statistical Significance**	
	Striatum	***Mean QA***	***Striatum***	***Mean QA***	***Striatum***	***Mean QA***
Left*	*3.24 ± 0.26*	*4.9 ± 0.9 (x10^{-3})*	*1.88 ± 0.25*	*4.1 ± 0.7 (x10^{-3})*	*$t = 20.9$; $p < 10^{-6}$*	*$t = 3.9$; $p = 3x\,10^{-4}$*
Right†	*3.20 ± 0.26*	*5.1 ± 0.9 (x10^{-3})*	*2.06 ± 0.33*	*3.2 ± 0.8 (x10^{-3})*	*$t = 14.9$; $p < 10^{-6}$*	*$t = 3.2$; $p = 0.002$*
Left vs. Right Statistical ‡ Significance	*$t = 1.8$; $p = 0.07$*	*$t = -3.85$; $p = 0.002$*	*$t = -5.3$; $p = 10^{-5}$*	*$t = -6.9$; $p < 10^{-6}$*		

*Left (right†) hemisphere in the PD group = hemisphere clinically most (least) affected in PD patients.

‡ statistical significance between hemispheres within the group.

Customized template for fiber tracking

A group average template was constructed from 62 control subjects (age=64.6 ±9.8 years; 31 females and 31 males). A DTI diffusion scheme was used, and 15 diffusion sampling directions were acquired. The b-value was 800 s/mm^2. The in-plane resolution was 1.75 mm. The slice thickness was 2 mm. The b-table was checked by an automatic quality control routine to ensure accuracy. The diffusion data were reconstructed in the MNI space using q-space diffeomorphic reconstruction (see reference *8* in the main text) to obtain the spin distribution function. A diffusion sampling length ratio of 1.25 was used. The diffusion was quantified using restricted diffusion imaging (see *32* in the main text). A deterministic fiber tracking algorithm (see *18* in the main text) was used, with a seeding region placed at the whole brain. The QA threshold was randomly selected. The angular threshold was randomly selected from 15 degrees to 90 degrees. The step size was randomly selected from 0.5 voxel to 1.5 voxels. The fiber trajectories were smoothed by averaging the propagation direction with a percentage of the previous direction. The percentage was randomly selected from 0% to 95%. Tracks with length shorter than 30 or longer than 300 mm were discarded. A total of 100,000 seeds were placed.

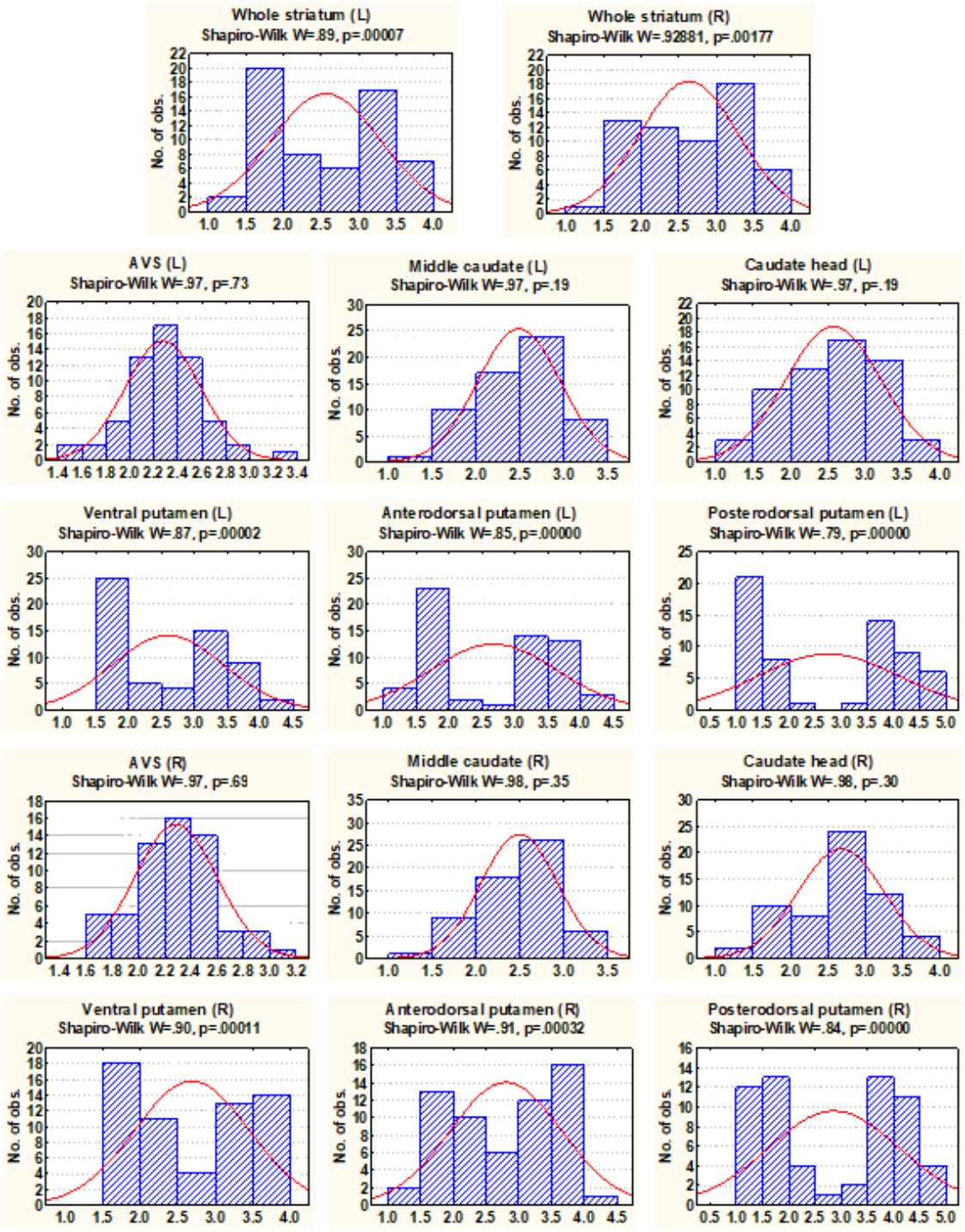

Supplementary Figure 1. Histograms of the whole striatum and sub-regions in the left (L) and right (R) hemispheres in the combined group. Only the anteroventral striatum (AVS), and caudate nucleus sub-regions showed normal distributions. The other sub-regions and the whole striatum also had more than one peak.

Supplementary Table 1. Pearson correlation coefficients and p-values between the whole striatum and sub-regions in each hemisphere in the combined group

Left*	**AVS**	**Middle caudate**	**Caudate head**	**Ventral putamen**	**Anterodorsal putamen**	**Posterodorsal putamen**
Whole striatum	*0.81*	*0.90*	*0.93*	*0.98*	*0.99*	*0.97*
	$p<10^{-6}$	$p<10^{-6}$	$p<10^{-6}$	$p<10^{-6}$	$p<10^{-6}$	$p<10^{-6}$
Right						
Whole striatum	*0.80*	*0.82*	*0.91*	*0.98*	*0.98*	*0.96*
	$p<10^{-6}$	$p<10^{-6}$	$p<10^{-6}$	$p<10^{-6}$	$p<10^{-6}$	$p<10^{-6}$

*The left hemisphere refers to the hemisphere clinically most affected in PD patients.

Supplementary Table 2. Pearson correlation and p-values between the whole striatum and sub-regions in each hemisphere in the control group.

Left*	**AVS**	**Middle caudate**	**Caudate head**	**Ventral putamen**	**Anterodorsal putamen**	**Posterodorsal putamen**
Whole striatum	*0.76*	*0.80*	*0.86*	*0.85*	*0.90*	*0.93*
	$p<10^{-6}$	$p<10^{-6}$	$p<10^{-6}$	$p<10^{-6}$	$p<10^{-6}$	$p<10^{-6}$
Right						
Whole striatum	*0.77*	*0.86*	*0.88*	*0.84*	*0.78*	*0.93*
	$p<10^{-6}$	$p<10^{-6}$	$p<10^{-6}$	$p<10^{-6}$	$p<10^{-6}$	$p<10^{-6}$

Supplementary Table 3. Pearson correlation and p-values between the whole striatum and sub-regions in each hemisphere in the PD group.

Left	**AVS**	**Middle caudate**	**Caudate head**	**Ventral putamen**	**Anterodorsal putamen**	**Posterodorsal putamen**
Whole striatum	*0.86*	*0.92*	*0.93*	*0.90*	*0.87*	*0.67*
	$p<10^{-6}$	$p<10^{-6}$	$p<10^{-6}$	$p<10^{-6}$	$p<10^{-6}$	$p<10^{-6}$
Right						
Whole striatum	*0.84*	*0.90*	*0.92*	*0.94*	*0.93*	*0.75*
	$p<10^{-6}$	$p<10^{-6}$	$p<10^{-6}$	$p<10^{-6}$	$p<10^{-6}$	$p<10^{-6}$

*The left hemisphere refers to the hemisphere clinically most affected in PD patients.

Supplementary Table 4. Coefficient of variation (*CoV)*, mean and standard deviation (*Std. Dev.)* of the whole striatum and sub-regions in the left and right hemispheres in the combined group.

	CoV. (%)		***Mean***		***Std. Dev.***	
	Left*	Right	Left*	Right	Left*	Right
Whole striatum	*28.52*	*24.71*	*2.56*	*2.63*	*0.73*	*0.65*
AVS	*14.04*	*13.54*	*2.28*	*2.29*	*0.32*	*0.31*
Middle caudate	*18.88*	*17.67*	*2.49*	*2.49*	*0.47*	*0.44*
Caudate head	*24.90*	*21.72*	*2.57*	*2.67*	*0.64*	*0.58*
Ventral putamen	*32.69*	*28.25*	*2.60*	*2.69*	*0.85*	*0.76*
Anterodorsal putamen	*35.82*	*30.36*	*2.68*	*2.80*	*0.96*	*0.85*
Posterodorsal putamen	*48.91*	*43.71*	*2.76*	*2.86*	*1.35*	*1.25*

*The left hemisphere refers to the hemisphere clinically most affected in PD patients.

Supplementary Table 5. Coefficient of variation (*CoV)*, mean and standard deviation (*Std. Dev.)* of the whole striatum and sub-regions in the left and right hemispheres in the control group.

	CoV (%)		***Mean***		***Std. Dev.***	
	Left	Right	Left	Right	Left	Right
Whole striatum	*8.02*	*8.13*	*3.24*	*3.2*	*0.26*	*0.26*
AVS	*9.27*	*9.76*	*2.48*	*2.46*	*0.23*	*0.24*
Middle caudate	*9.51*	*12.79*	*2.84*	*2.19*	*0.27*	*0.28*
Caudate head	*13.03*	*14.05*	*3.07*	*2.42*	*0.4*	*0.34*
Ventral putamen	*10.32*	*10.04*	*3.39*	*2.79*	*0.35*	*0.28*
Anterodorsal putamen	*7.80*	*9.70*	*3.59*	*2.99*	*0.28*	*0.29*
Posterodorsal putamen	*9.58*	*11.40*	*4.07*	*3.42*	*0.39*	*0.39*

Supplementary Table 6. Coefficient of variation (*CoV)*, mean and standard deviation (*Std. Dev.)* of the whole striatum and sub-regions in the left and right hemispheres in the PD group.

	CoV (%)		***Mean***		***Std. Dev.***	
	Left*	Right	Left*	Right	Left*	Right
Whole striatum	*13.30*	*16.02*	*1.88*	*2.06*	*0.25*	*0.33*
AVS	*12.08*	*13.74*	*2.07*	*2.11*	*0.25*	*0.29*
Middle caudate	*15.96*	*19.47*	*2.13*	*2.26*	*0.34*	*0.44*
Caudate head	*19.50*	*21.26*	*2.41*	*2.07*	*0.47*	*0.44*
Ventral putamen	*10.50*	*14.07*	*1.81*	*1.99*	*0.19*	*0.28*
Anterodorsal putamen	*15.82*	*19.70*	*1.77*	*2.03*	*0.28*	*0.4*
Posterodorsal putamen	*13.10*	*20.96*	*1.45*	*1.67*	*0.19*	*0.35*

*The left hemisphere refers to the hemisphere clinically most affected in PD patients.

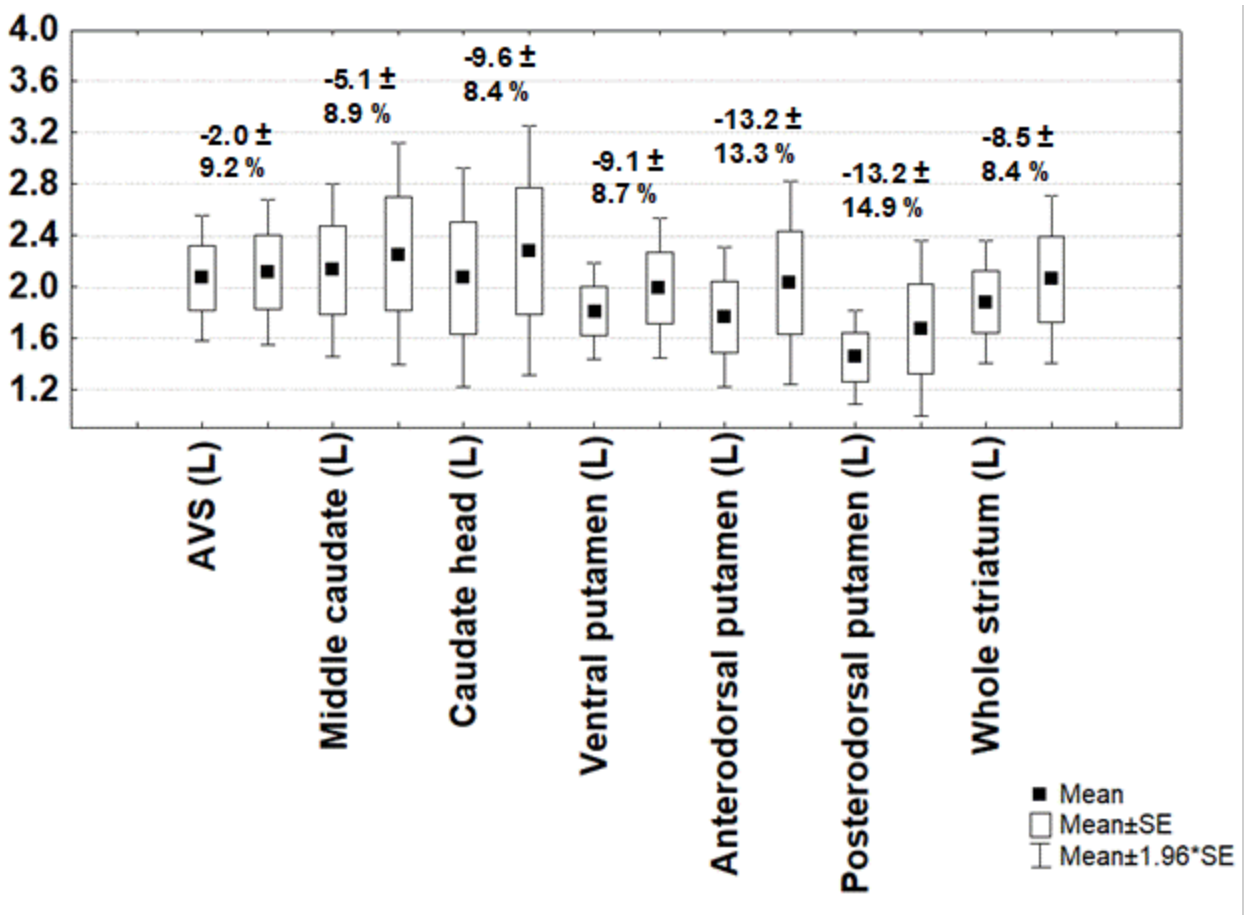

Supplementary Figure 2. Left-right asymmetry of ^{11}C-DTBZ DVR in the whole striatum and sub-regions in the PD group. Mean (± SD, in percent) asymmetry indices (AI) are shown at the top of the figure. AI = 100 x (left - right) / ((left + right) x 0.5). The anteroventral striatum (AVS) showed the lowest mean asymmetry. The left hemisphere refers to the hemisphere clinically most affected in PD patients.

Supplementary Table 7. Shapiro-Wilk W statistic (and p-values) for all main study variables in the left and right hemispheres.

	PD group		Control group		Combined group	
	Left*	***Right***	***Left***	***Right***	***Left****	***Right***
AVS	0.96 (0.29)	0.96 (0.30)	0.94 (0.07)	0.95 (0.12)	0.97 (0.73)	0.97 (0.69)
Whole striatum	0.98 (0.85)	0.94 (0.76)	0.98 (0.69)	0.94 (0.10)	-	-
Mean QA	0.98 (0.79)	0.97 (0.43)	0.97 (0.62)	0.97 (0.55)	0.98 (0.28)	0.97 (0.21)
Mean QA (PD)†	0.94 (0.09)	0.94 (0.08)	-	-	-	-
Mean QA-LOO	0.97 (0.44)	0.97 (0.58)	-	-	-	-
Mean FA	0.96 (0.33)	0.97 (0.57)	0.97 (0.60)	0.98 (0.87)	0.97 (0.27)	0.98 (0.59)
Mean FA (PD)‡	-	0.97 (0.40)	-	-	-	-
Bradykinesia sub-score	0.96 (0.33)		-		-	

*The left hemisphere refers to the hemisphere clinically most affected in PD patients. Mean QA (PD)† and mean FA (PD)‡ are the respective values by using tract templates estimated in the PD group separately. AVS = Anteroventral striatum. LOO = leave-one-out.

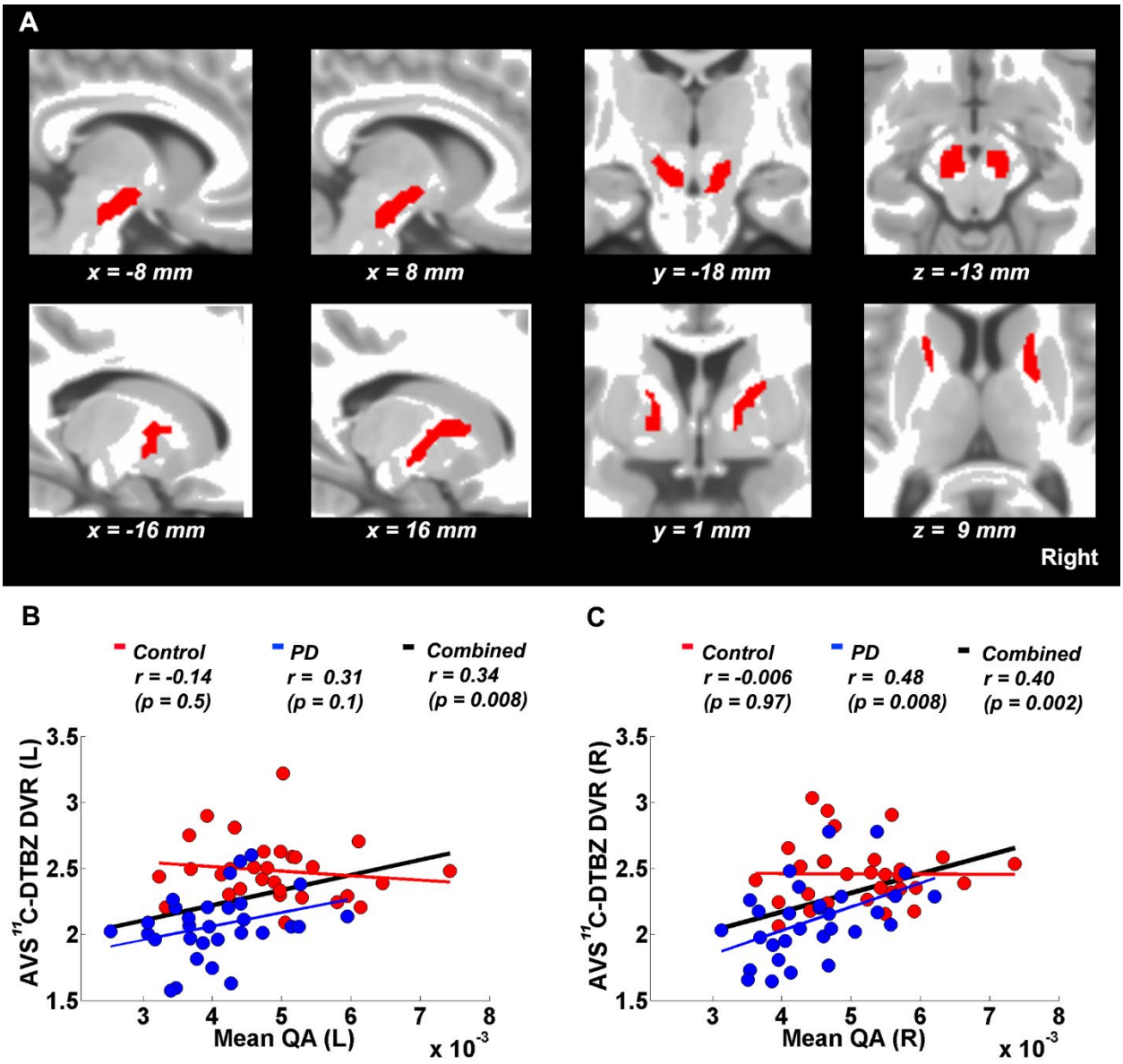

Supplementary Figure 3. (A) Tract templates identified in the combined group (overlaid on a T1-weighted MR image in MNI space). Tract templates followed similar paths to those observed in the PD group, but with higher volumes (left = 2.02 cm^3; right= 2.6 cm^3). **(B)** The mean QA (across the tract template) positively correlated with anteroventral striatum (AVS) ^{11}C-DTBZ DVR in the left hemisphere (black regression line). Analyses in separate groups (using the combined group tract template) showed no significant correlation in the control group (red line and circles) nor the PD group (blue regression line and circles). **(C)** The same as (B) for the right hemisphere, but unlike (A), a significant correlation was observed in the PD group. These analyses showed that the correlation found in the combined group was mainly influenced by the

PD group, making separate PD group analysis more appropriate, especially for cross-validation. However, the combined group analysis allowed us to have mean QA estimates for each hemisphere and group using the same templates for comparison of mean QA between PD and control groups. The left hemisphere in the PD group refers to the hemisphere clinically most affected in PD patients.

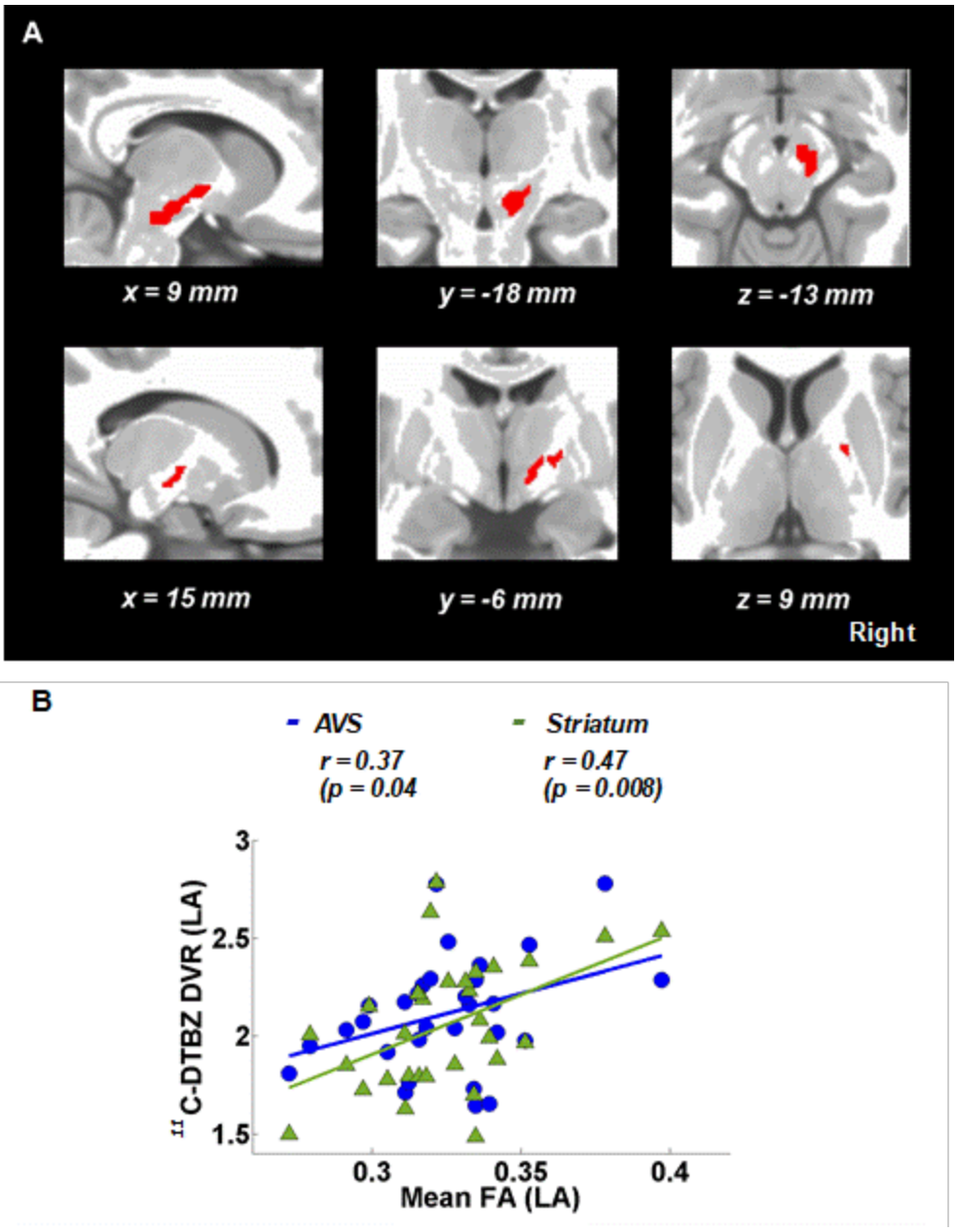

Supplementary Figure 4. (A) FA tract template identified in the PD group in the least affected (LA) hemisphere (overlaid on a T1-weighted MR image in the MNI space). No tract template was identified in the most affected hemisphere. **(B)** The mean FA (across the PD template) positively correlated with anteroventral striatum (AVS) (blue regression line and circles) and the whole striatum ^{11}C–DTBZ DVR values (green regression line and triangles) in the LA

hemisphere. Note that the correlation with the whole striatum ^{11}C–DTBZ DVR values was lower compared with mean QA in the same hemisphere (Figs 1.C in the main text). The right hemisphere in the PD group refers to the hemisphere clinically least affected.

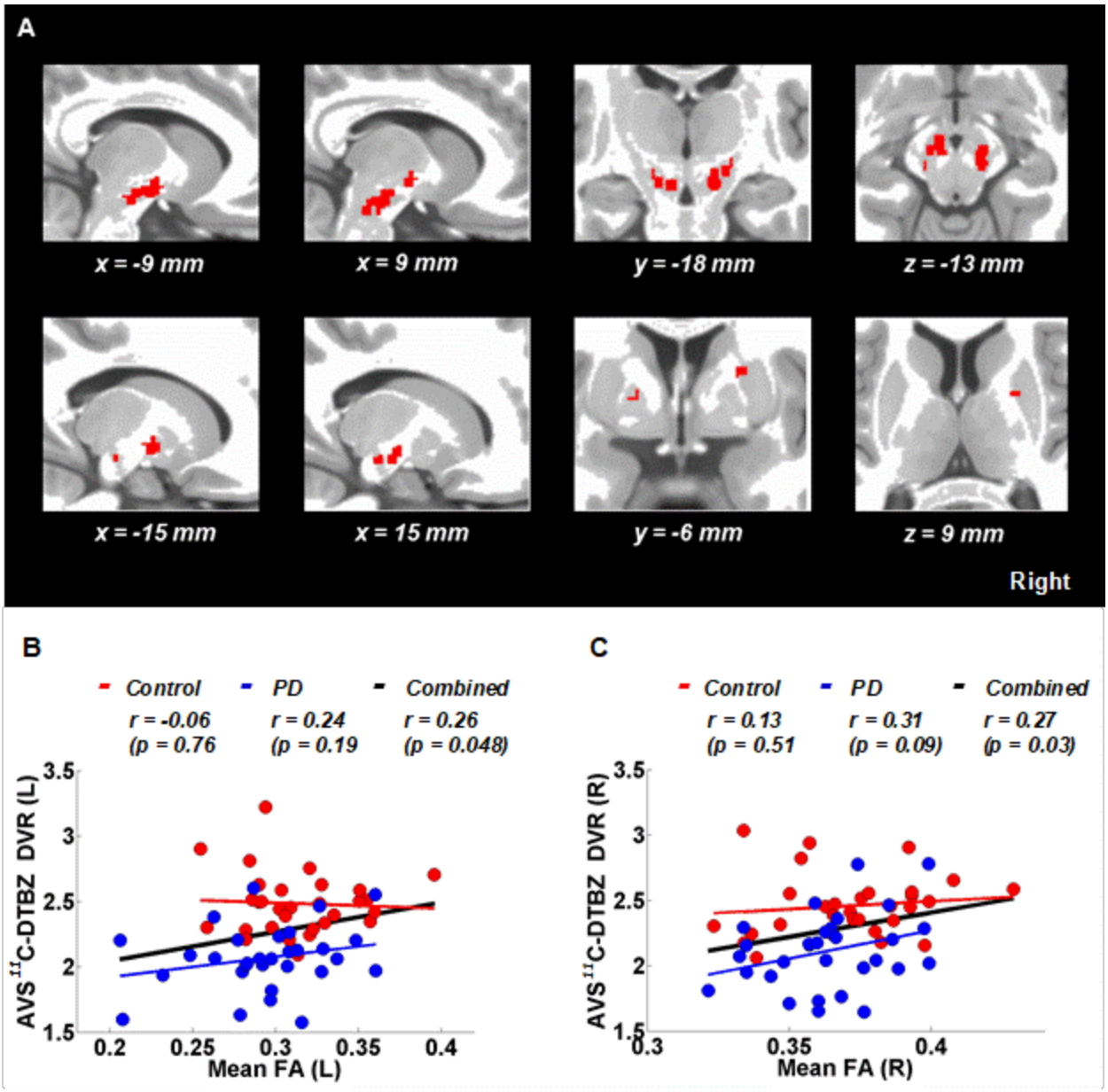

Supplementary Figure 5. (A) Tract templates identified in the combined group using the FA index (overlaid on a T1-weighted MR image in the MNI space). The tracts follow trajectories somewhat similar to those identified using QA but more fragmented and with volumes more than 50% smaller in both hemispheres (left = 0.92 cm^3; right = 1 cm^3). **(B)** The mean FA (across the tract template) positively correlated with anteroventral striatum (AVS) ^{11}C-DTBZ DVR in the left hemisphere (black regression line). Analyses in the separate groups (using the combined group tract template) showed no significant correlation in the control group (red regression line and circles) nor in the PD group (blue regression line and circles). **(C)** The same as (B) for the

right hemisphere. The left hemisphere in the PD group refers to the hemisphere clinically most affected in PD patients.

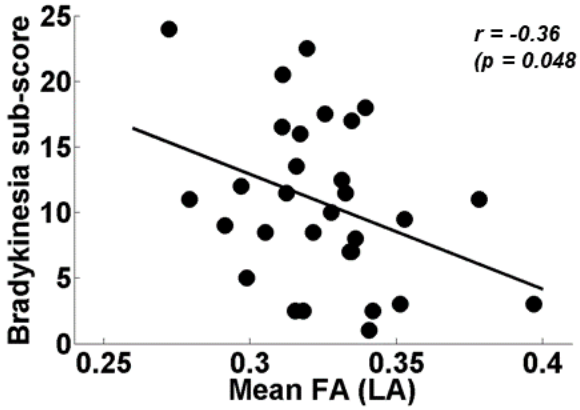

Supplementary Figure 6. Mean FA in the LA hemisphere was significantly negatively correlated with the MDS-UPDRS bradykinesia sub-score of PD subjects but the correlation coefficient was lower compared to the correlation found with the mean QA and mean QA-LOO for that hemisphere (Fig, 3.B and 3.D in the main text). The right hemisphere in the PD group refers to clinically least affected.

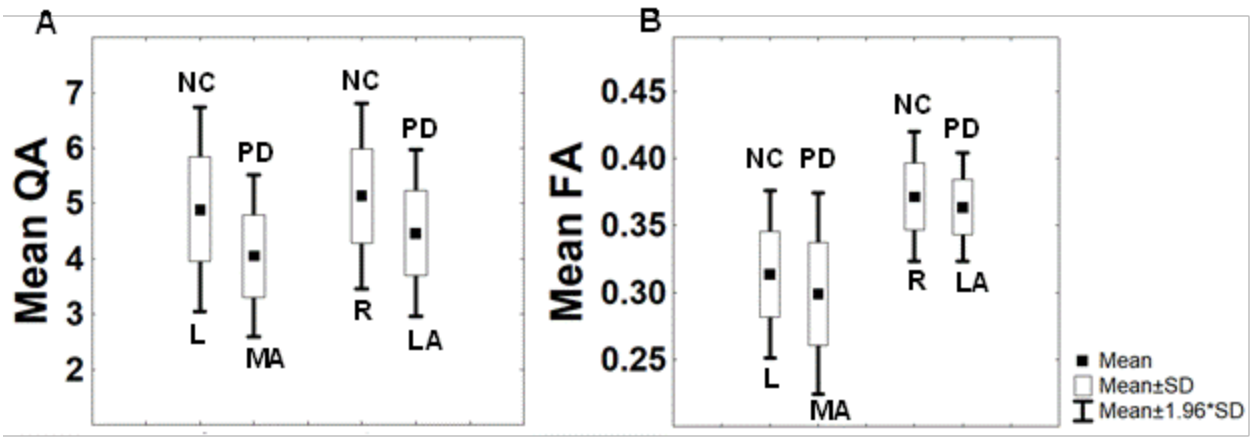

Supplementary Figure 7. (A) Control group versus PD group showed significant differences of the mean QA in both hemispheres (see also Table 4 in main text). The mean QA across the PD patients in the LA hemisphere was also significantly higher compared with the mean QA in the MA hemisphere (see also Table 4 in main text). **(B)** In contrast, the mean FA showed no significant differences between groups (Control left: 0.31± 0.03, PD left: 0.30 ± 0.04, t=1.58, p=0.12; Control right: 0.37± 0.02, PD right: 0.36 ± 0.02, t=1.34, p=0.18). As the mean QA, there were significant differences between hemispheres in the control group (t= -11. 9, $p < 10^{-6}$) due to the differences between the left and right tract templates of the combined group (Supplementary Fig. 5.A) applied to the control group. With mean FA this effect was also more noticeable compared to mean QA **(A)**. The right hemisphere in the PD group refers to the hemisphere clinically least affected in PD patients.